Multifunctional lanthanide and silver ions co-doped nano-chlorapatites with combined spectroscopic and antimicrobial properties

R.J. Wiglusz[1,], Z. Drulis-Kawa[2], R. Pązik[1], K. Zawisza[1], A. Dorotkiewicz-Jach[2], J. Roszkowiak[2], J.M. Nedelec[3,4]*

[1] *Institute of Low Temperature and Structure Research, Polish Academy of Sciences, Okolna 2, 50-422 Wroclaw, Poland*
[2] *Institute of Genetics and Microbiology, University of Wroclaw, Przybyszewskiego 63/77, 51-148 Wroclaw, Poland*
[3] *Clermont Université, ENSCCF, ICCF, BP10448, 63000 Clermont-Ferrand, France.*
[4] *CNRS, UMR 6296, ICCF, 63171 Aubière, France.*

Abstract

Nanocrystalline chlorapatites ($Ca_{10}(PO_4)_6Cl_2$) doped with lanthanide ions (Eu^{3+}, Er^{3+} and Yb^{3+}) and co-doped with silver ions (Ag^+) were synthesized by hydrothermal synthesis route. XRD, TEM, and SAED measurements indicated that the powders are single phased and crystallize with an hexagonal structure with good dispersion. The results showed well crystallized chlorapatite grains with diameter of about 45 nm.

The antimicrobial activity of the nanoparticles against: *Escherichia coli* ATCC11229 and ATCC25922, and *Klebsiella pneumoniae* ATCC 700603, *Pseudomonas aeruginosa* PAO1 and ATCC27853 were studied. The best activity was observed for $Eu^{3+},Ag^+:Ca_{10}(PO_4)_6Cl_2$ and $Eu^{3+},Ag^+,Yb^{3+}:Ca_{10}(PO_4)_6Cl_2$ compositions. These multifunctional nanocrystalline powders could be used as a promising antimicrobial agent and material for bio-detection.

Keywords: Chlorapatites, Lanthanide and Silver ions, Antimicrobial, Nanoparticles.

[*]Corresponding author:

E-mail: R.Wiglusz@int.pan.wroc.pl

Phone: +48-71-395-41-59

Fax: +48-71-344-10-29

1. Introduction

Chlorapatites do not occur naturally on Earth in pure form, can be found in astral bodies such as meteorities[1]. Structure of this material depends on thermal conditions as stoichiometric compound $Ca_{10}(PO_4)_6Cl_2$ crystallizes with monoclinic space group $P2_1/b$ evolves towards hexagonal group (space group $P6_3/m$), when heated above 350°C[2,3]. The chlorapatite unit cell contains ten calcium cations in two distinct crystallographic sites, six phosphate and two chlorine anions lying on the crystallographic c-axis perpendicular to the plane defined by three calcium ions at $z = 0$ and $z = \frac{1}{2}$. Two calcium positions (Ca_1 and Ca_2) possess quite different stereochemical environment. The coordination poly of the Ca_1 position is a $[CaO_9]$ tricapped trigonal prism and the environment of the Ca_2 position is the $[CaO_6Cl]$ irregular polyhedron formed by hemisphere of 6 oxygen atoms capped by the volatile anion components[4].

Chlorapatite has many different applications. For instance if doped with metal cations such as rare earth elements (RE^{3+}, RE^{2+}) it can be used as a phosphor material in optoelectronic applications[5] as well as more sophisticated directions like bio-detection[6]. It is worth to note that the rare earth cations can enter two different positions substituting Ca^{2+} with some site preference driven by their concentration and reaction conditions. However, this material can also exhibit antibacterial properties when doped with silver ions[7]. Chlorapatite composites can be of great interest as the development of antibiotic resistance in almost all clinically important pathogens became serious therapeutic problem in recent decades. The Gram-negative bacteria such as pseudomonads and enterobacteria became multidrug/pandrug resistant (MDR/PDR) to conventional antibiotics enforcing urgent development of alternative and efficient antibacterial treatment[8]. One of the most promising strategies that helps to overcome problems with colonization and infection development by severe pathogens is the application of modern bionanomaterials. Current technologies allows to obtain new bionanomaterials applicable in medicine especially as components of permanent implants or short-term biomedical devices which are prone to bacterial colonization. Such proceedings

[1] K. Lodders, B. Fegley, Jr. The Planetary Scientist's Companion; Oxford University Press: Oxford, 1998.

[2] H.B. Vanrees, M. Mengeot, E. Kostiner, Mater. Res. Bull., 1973, 8, 1307.

[3] H. Suda, M. Yashima, M. Kakihana, M. Yoshimura, J. Phys. Chem., 2002, 99, 6754.

[4] S. Naray-Szabo. Z. Kristallogr., 1930,75, 387.

[5] N. Murase, R. Jagannathan, Y. Kanematsu, Y. Kawasaki, A. Tomita, T. Yazawa, T. Kushida, J. Lum., 2000, 87-89, 488

[6] H. Zhang, X.J. Ye, J.S. Li, Biomed Mater., 2009, 4, 45007.

[7] R.J. Wiglusz, A. Kedziora, A. Lukowiak, W. Doroszkiewicz, W. Strek, J. Biomedical Nanotech., 2012, 8, 605.

[8] M. Bassetti, M. Merelli, C. Temperoni, A. Astilean, Ann Clin. Microbiol. Antimicrob. 2013, **12**:22.

prevents bacterial adhesion and lengthens utility of medical devices[9]. Modern bionanomaterials containing metal ions protects organism against adverse reaction of pathogenic bacteria and may be used with success in prevention against bacterial infections especially those connected with biofilm formation. Bionanomaterial composites may also be applied as part of therapy against pathogens causing skin infections[10].

Bactericidal effect of chlorapatite doped with different metal ions is the subject of the present work.

2. Experimental

2.1. Synthesis of the samples ($Ca_{10}(PO_4)_6Cl_2$ nanoparticles doped with Eu^{3+}, Yb^{3+}, Ag^+, Eu^{3+}/Ag^+, $Eu^{3+}/Ag^+/Yb^{3+}$ and $Er^{3+}/Ag^+/Yb^{3+}$ ions).

A detailed synthesis of the $Ca_{10}(PO_4)_6Cl_2$ nanoparticles using microwave hydrothermal technique was described by the authors elsewhere[11]. The concentration of dopants and co-dopants was set as a fixed 2 mol% with respect to the Ca^{2+} overall content. Therefore, in the case of the single ion doping (Eu^{3+}, Yb^{3+} and Ag^+) their quantities were set at 2 mol% whereas samples co-doped with europium and silver ions contained 2 mol% of Eu^{3+} and 2 mol% of Ag^+ (4 mol% in total) and finally triply doped samples ($Eu^{3+}/Ag^+/Yb^{3+}$ and $Er^{3+}/Ag^+/Yb^{3+}$) contained 6 mol% of dopants in total (see Table 1 for composition).

Stoichiometric amounts of rare earth (RE) oxides Eu_2O_3 (99.99 % Alfa Aesar), Yb_2O_3 (99.99 % Alfa Aesar), Er_2O_3 (99.99% Alfa Aesar) were digested in excess of HNO_3 (ultrapure Avantor Poland) in order to transform RE^{3+} oxide into the water soluble RE^{3+} nitrates every time prior to the final preparation steps. Typical procedure involved dissolving and mixing using magnetic stirrer stoichiometric amounts of the RE^{3+} nitrates and when necessary $AgNO_3$ (99.995 % Alfa Aesar) together with the $Ca(NO_3)_2 \cdot 4H_2O$ (99.995 % Alfa Aesar) in MQ-water. The last step of the formation of by-product involved addition of the $(NH_4)_2HPO_4$ (99.99% Sigma Aldrich) and NH_4OH (99 % Avantor Poland) resulting in fast precipitation of the ultra-fine powder. Final suspension containing by-product being a mixture of the amorphous and crystalline phase of the $Ca_{10}(PO_4)_6Cl_2$ was placed in the microwave reactor (ERTEC MV 02-02). After 90 min of the microwave stimulated hydrothermal processing at 200°C and under autogenous pressure of 50 atm. white powder was obtained, washed with de-

[9] J. Fernebro, Drug Resist. Updat., 2011, **14**, 125.

[10] R.Y. Pelgrift, A.J. Friedman , Adv. Drug Deliv. Rev., 2013, **65**, 1803.

[11] R. Pązik, J.M. Nedelec and R.J. Wiglusz, CrystEngComm, 2014, 16, 5308.

ionized water and dried at 60^oC for 24 h. In order to get rid of amorphous phase and any residual or un-reacted substrates a final thermal treatment at 800^oC was applied.

2.2. Bacterial strains.

Five reference strains of Gram- negative bacilli from the American Type Culture Collection were used: *Pseudomonas aeruginosa* ATCC 27853, *Pseudomonas aeruginosa* PAO1, *Escherichia coli* ATCC 11229, *Escherichia coli* 25922 and *Klebsiella pneumoniae* 700603. Bacteria were stored at -70℃ in Trypticase Soy Broth (Becton Dickinson and Company, Cockeysville, MD, USA) supplemented with 20% glycerol.

2.3. Determination of bacterial susceptibility.

The antimicrobial activity of the $Ca_{10}(PO_4)_6Cl_2$ nanoparticles against five reference strains were performed by microdilution method according to EUCAST recommendations[12]. The tests were performed by a saline microdilution method. Concentration of 1%, 0.1%, 0.01%, 0,0005% and 0,00005% of $Ca_{10}(PO_4)_6Cl_2$ doped with different ions were prepared in saline solution at physiological pH=7.4 and sterilized. Immediately after preparation, 200 μl of each of diluted sample were placed into microtitration wells. For the experiments, bacterial strains were inoculated onto blood agar plates, incubated for 18 h at 37℃, and then diluted in saline to the optical density equal to the McFarland No. 0.5. Ten μl of bacterial culture was diluted 1:10 (approximate concentration: 10^7 cfu/ml) and added to the microtitration wells containing the apatite dilution. The final concentration of microorganisms was $5x10^5$ cfu/ml. The plates were incubated for 18 h at 37℃ with continuous shaking. Positive controls (100% survival rate) consisted of bacteria inoculated in saline solution. Negative controls (sterility) consisted of non-inoculated apatite dilutions in saline. Each assay was repeated in triplicate at three different times to ensure reproducibility of results. The number of colony forming units (cfu/ml) was determined after incubation and compared to positive control evaluated as 100% of survival rate.

2.4. Powders characterization.

The X-ray diffraction (XRD) patterns were measured in a 2θ range of 10 – 60 ^{o} with a X'Pert Pro PANalytical X-ray diffractometer (Cu, Kα1: 1.54060 Å). The powders were investigated by Transmission Electron Microscopy (TEM) using Philips CM-20 SuperTwin microscope, operating at 200 kV. Specimens for HRTEM were prepared by dispersing small amount of sample in methanol and putting a droplet of the suspension on a copper microscope

---

[12] The European Committee on Antimicrobial Susceptibility Testing - EUCAST 2014

grid covered with perforated carbon. The concentration of silver was determined by Inductively Coupled Plasma Atomic Emission Spectrometry (ICP-AES) after digesting each sample in nitric acid.

3. Results and Discussion

3.1. Structural analysis.

The phase purity and structure of the various $Ca_{10}(PO_4)_6Cl_2$ samples were checked by XRD analysis.

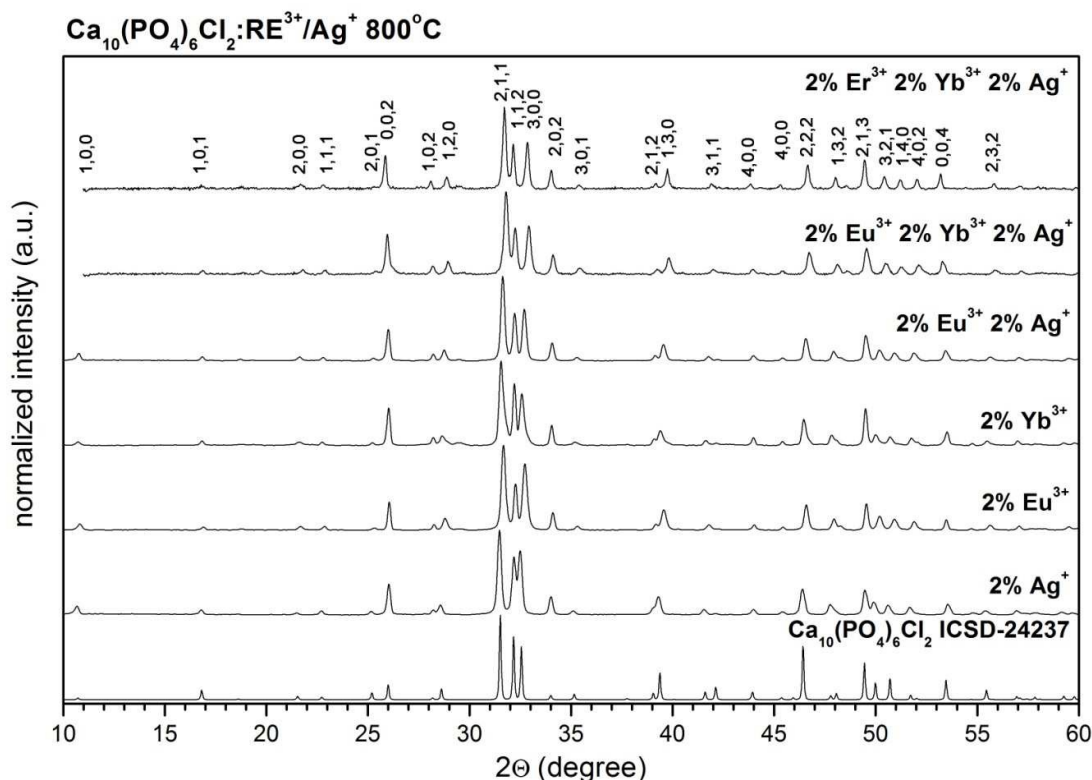Figure 1. XRD patterns of the $Ca_{10}(PO_4)_6Cl_2$ samples for various dopant types treated at 800°C.

As can be seen in Figure 1, all powders are fully crystallized and only peaks characteristic of the hexagonal $Ca_{10}(PO_4)_6Cl_2$ phase are present[13]. No straightforward effect of the different dopant can be observed. As no impurity phase related to doping ions is detected, it can be assumed that the prepared samples formed solid solutions with no secondary phase separation evidence. For a more detailed investigation of the structural features, the Rietveld refinement method was applied using Maud 2.33[14]. The quality of structural refinement was verified by R-values (R_{wnb}, R_b, R_{exp}, R_w). Moreover, other parameters with additional

---

[13] Card No. 24237 ICDS, Fachinformationszentrum Karlsruhe, 2012.
[14] L. Lutterotti, S. Matthies, Mater. Sci. Forum, 2002, 408, 1603.

functions were applied to find a structural refinement with better quality and reliability. The optimized parameters were: scale factor, background with exponential shift, exponential thermal shift and polynomial coefficients, basic phase, microstructure, crystal structure, size strain (anisotropic, no rules), structure solution model (genetic algorithm SDPD), shift lattice constants, profile half-width parameters (u, v, w), texture, lattice parameters (a, b, c), factor occupancies and atomic site occupancies (Wyckoff). The crystal structure data of the $Ca_{10}(PO_4)_6Cl_2$ single crystal with hexagonal structure was used as reference standard[13]. Figure 2 shows an excellent agreement between the observed XRD pattern and the theoretical fitting results of the representative $Ca_{10}(PO_4)_6Cl_2$: 2% Eu^{3+}. This indicates the validity of the Rietveld refinement method as attested very small differences in the intensity scale as illustrated by the (Y_{obs} - Y_{calc}) plot. More details regarding Rietveld refinement are displayed in Tables 1 and 2 as well as in the Figure 3. Moreover, it is further expected that the increase of the dopants amount above a certain critical level would lead to multiphase products. Additionally, due to RE^{3+} ionic radii similarity with Ca^{2+} ions, assumption can be made that both Ca^{2+} crystallographic sites would be occupied by Eu^{3+}, Yb^{3+} and Er^{3+} ions and Ag^+ (Ca^{2+} (CN_9) - 1.18 Å, Eu^{3+} (CN_9) - 1.12 Å, Er^{3+} (CN_9) - 1.062 Å, Yb^{3+} (CN_9) - 1.042 Å, Ag^+ (CN_9) > 1.28 Å, Ca^{2+} (CN_7) - 1.06 Å, Eu^{3+} (CN_7) - 1.01 Å, Er^{3+} (CN_7) - 0.945 Å, Yb^{3+} (CN_7) - 0.925 Å, Ag^+ (CN_7) - 1.22 Å)[15]. The issue of exact site preference of the RE^{3+} in the $Ca_{10}(PO_4)_6Cl_2$ matrix was already discussed[8,16].

[15] R.D. Shannon, Acta Cryst., **1976**, *A32*, 751.
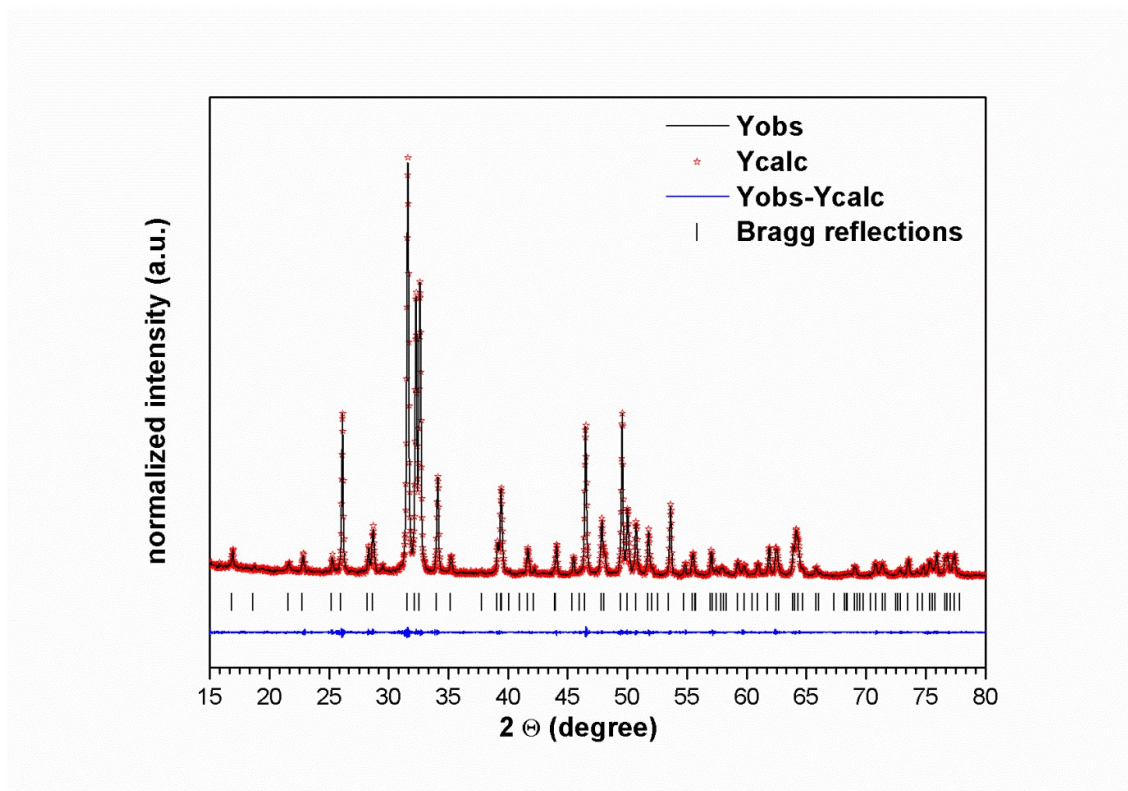[16] M. Fleet, X. Liu, Y. Pan, *Am. Miner.*, **2000**, *85*, 1437.

Figure 2. Representative results of the $Ca_{10}(PO_4)_6Cl_2$:2% Eu^{3+} Rietveld analysis (red – fitted diffraction; blue – differential pattern, vertical lines – reference phase peak position).
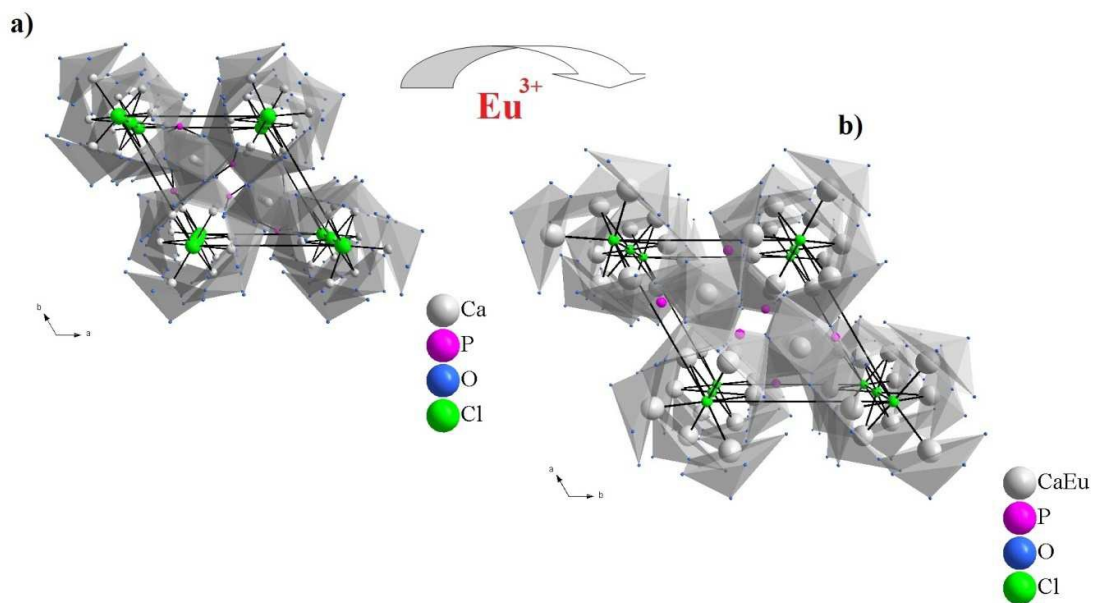

Figure 3. Projection of the $Ca_{10}(PO_4)_6Cl_2$ unit cell with indication of the Ca^{2+} as well as Ca^{2+}/Eu^{3+} and P^{5+} coordination polyhedra.

Table 1. Unit cell parameters (a,c), cell volume (V), grain size as well as refine factor (R_W) for the $Ca_{10}(PO_4)_6Cl_2$ powder as function of different dopants.

Samples	a [Å]	c [Å]	V [Å³]	R. grain size [nm]	R_w [%]
single crystal	9.52(3)	6.85(3)	537.64(3)	–	–
2% Ag^+	9.43(5)	6.88(4)	529.83(7)	50	1.21
2% Eu^{3+}	9.57(1)	6.84(4)	542.59 (5)	70	1.13
2% Yb^{3+}	9.52(2)	6.85(4)	537.64(4)	65	1.35
2% Eu^{3+},2% Ag^+	9.49(3)	6.86(1)	535.04(1)	85	1.95
2% Eu^{3+}, 2%Yb^{3+}, 2% Ag^+	9.43(9)	6.87(9)	529.06(7)	66	1.63
2% Er^{3+}, 2%Yb^{3+}, 2% Ag^+	9.43(5)	6.88(4)	529.83(7)	70	1.73

Table 2. Atomic parameters for $Eu_{0.02}Ca_{0.98}(PO_4)_6Cl_2$ annealed at 800°C.

Sample	$Eu_{0.02}Ca_{0.98}(PO_4)_6Cl_2$, Z = 2
Space group	Hexagonal $P6_3/m$ (No. 176)
Calculated cell parameters	a = 9.57(6) Å b=6.84(4) V = 542.59(5) Å³
R_w	1.13 %
R_{wnb}	1.25 %
R_{all}	0.88 %
R_{nb}	1.01 %

Selected contacts	
Ca|Eu − Eu|Ca	3.42(2) Å
Ca|Eu − O	2.3212(1) Å
P − P	4.6600(1) Å
P − O	1.6021(7) Å
O − P − O	110.818(2) °

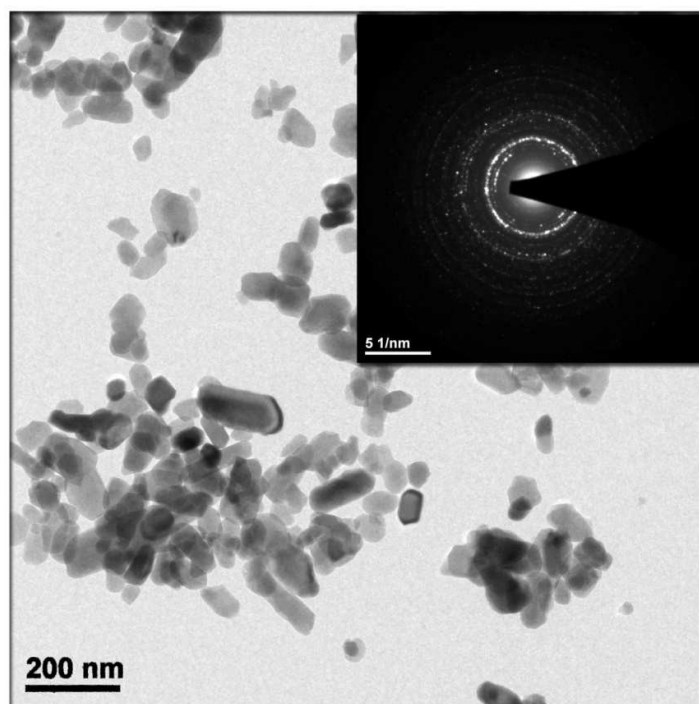| Atom	Wyckoff positions	x	y	z	B_{iso}	Occ. (<1)
Ca1	*4f*	1/3	2/3	0.00443	0.89(4)	0.99
Ca2	*6h*	0.25358	0.99422	0.25012	0.91(3)	0.99
P1	*6h*	0.41176	0.37774	0.24955	1.03(1)	
O1	*6h*	0.33750	0.49275	0.24951	1.00(1)	
O2	*6h*	0.59903	0.47130	0.24952	1.00(1)	
O3	*12i*	0.34270	0.25979	0.06671	1.00(1)	
Cl1	*2b*	0.99999	0.00001	0.99950	0.92(1)	
Eu1	*4f*	1/3	2/3	0.00383	0.95(4)	0.01
Eu2	*6h*	0.25351	0.99410	0.25049	0.96(5)	0.01

Figure 4. TEM and SAED images of the representative $Ca_{10}(PO_4)_6Cl_2$: 2% Eu^{3+} sintered at 800^oC.

In accordance with TEM analysis (Figure 4) the $Ca_{10}(PO_4)_6Cl_2$ powder sample contains loosely agglomerated, regular and elongated particles. The particle size is around 60 nm with fairly broad size distribution. Taking into account that the last synthesis step involved thermal treatment at high temperature the resulting material must be agglomerated what directly causes multimodal sizes and is a typical image of such annealing directly connected with Ostwald ripening mechanism[17]. The spotty SAED pattern (Figure 4 inset) confirms the high degree of crystallization as well as measured distances between crystallographic planes are matching well reference standard of pure $Ca_{10}(PO_4)_6Cl_2$ phase.

3.2. Antibacterial activity of $Ca_{10}(PO_4)_6Cl_2$ nanoparticles

Five Gram-negative bacterial strains belonging to 3 species (*P. aeruginosa, E. coli and K. pneumoniae*) were treated with chlorapatites doped with different metal ions. Antibacterial properties were checked by indication of bacterial survival rate in the presence of serial concentrations of $Ca_{10}(PO_4)_6Cl_2$ (1%, 0.1%, 0.01%, 0,0005% and 0,00005%) doped and co-doped with silver, europium, ytterbium and erbium ions. The undoped $Ca_{10}(PO_4)_6Cl_2$ nanoparticle composition did not show antibacterial effect similarly as described for hydroxyapatites by Wiglusz R. J et al.[7].

---

[17]S. Abtmeyer, R. Pazik, R.J. Wiglusz, M. Małecka, G.A. Seisenbaeva, V.G. Kessler, *Inorg. Chem.*, **2014**, *53*, 943.
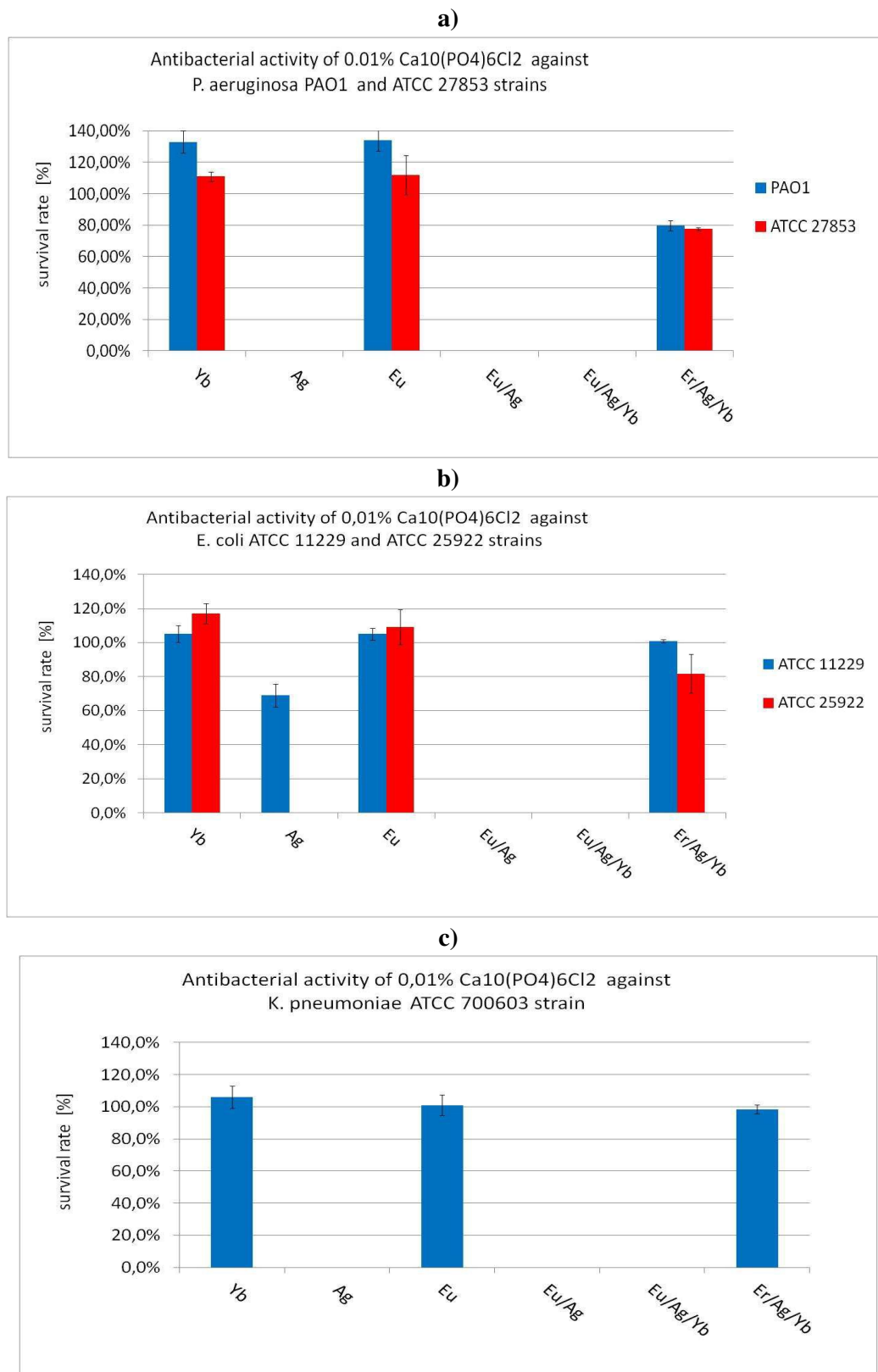
a)

b)

c)

Figure 5. Antibacterial activity of chlorapatite doped and co-doped with different rare earth ions and silver ions (Ag$^+$) against various bacteria strains.

The family of apatites with formula of $Ca_{10}(PO_4)_6Cl_2$ doped and co-doped with optically active cations like Eu^{3+} as well as Eu^{3+}/Yb^{3+}, and Yb^{3+}/Er^{3+} were synthesized for up-conversion fluorescence applications. These features combined with highly photostable luminescent properties of rare earth dopants and lack of OH^- group make the nanocrystalline chlorapatites highly attractive as luminescent bio-labels[18].

The lowest concentration exhibiting bacterial count reduction was established as 0.01%, thus the antibacterial activity comparison of different chlorapatite samples was made for this concentration (Figure 5). The bactericidal activity (100% reduction of colony count) was obtained for $Ca_{10}(PO_4)_6Cl_2$ containing Ag against all tested strains with one exception. In the case of *E. coli* ATCC 11229 strain survival rate was noted at 65%. In the case of higher concentrations tested (0,1%, 1%) the bactericidal effect was observed (data not shown). Similar results for hydroxyapatites doped with silver were obtained by Wiglusz R. J et al.[7]. On the other hand, a chloride ion is considered as substituent because of its biological significance. This relevance is connected with its ability to form an acidic environment on the bone surface and an activation of osteoclasts in the bone resorption processes[19].

The $Ca_{10}(PO_4)_6Cl_2$ doped with Yb^{3+} or Eu^{3+} alone, did not demonstrated any antibacterial effect, but even stimulation of bacterial culture growth was observed instead, as the survival rate exceeded 100%. Nevertheless the usage of Yb^{3+} or Eu^{3+} was rather connected with their luminescence properties than improvement of antibacterial properties, as in literature there are no evidence on bactericidal properties of those ions.

The non-toxic upconverting nanocrystalline phosphates are very promising for bio-imaging applications[20]. The NIR absorption minimizes photodamage of living cell as well as and allows deep tissue penetration[21]. Additionally, the elimination of autofluorescence as result of the upconversion phenomenon gives a possibility increases the detection of studied biomaterials. Conjunction of Eu^{3+} with Ag^+ brought synergistic effect against all tested strains giving 100% reduction of bacterial cells count in the sample. Conjunction of Eu^{3+}, Ag^+ supplemented with Yb^{3+}, which increased bacterial growth as a single ion, also allowed to obtain complete eradication of all tested bacteria. It seems that the antibacterial activity is related only to interactions between Eu^{3+}, Ag^+ ions. The ytterbium ion in $Eu^{3+}/Ag^+/Yb^{3+}$ composition should play role only as sensitizer of upconverting processes. The replacement of

[18] A. Doat, F. Pelle, N. Gardant, A. Lebugle, *J. Solid State Chem.*, **2004**, 1777, 1179.
[19] P.H. Schlesinger, H.C. Blair, S.L. Teitalbaum, J.C. Edwards, *J. Biol. Chem.*, **1997**, 272 (1997) 18636.
[20] F. Chen, Y. Zhu, J. Wu, P. Huang, and D. Cui, *Nano Biomed. Eng.*, **2012**, 4, 41.
[21] J. Rao, A. Dragulescu-Andrasi, H. Yao, *Curr. Opin. Biotechnol.*, **2007**, *18,* 17.

Eu^{3+} by Er^{3+} in the above chlorapatite composition dramatically changed the antibacterial properties from 100% to 0%-20% reduction of bacterial cell count, what confirm above assumption of Eu/Ag interaction. Nevertheless, the $Er^{3+}/Ag^+/Yb^{3+}$ composition exhibited better antibacterial activity against P. aeruginosa in comparison to *E.coli* and *K. pneumoniae* strains. Obtained results confirm preponderance of europium in antibacterial applications, but only as synergistic correlation with Ag^+, as crucial element for bactericidal activity enhancing. Similar results were previously confirmed by Wiglusz et al. in case of hydroxyapatites doped with silver and europium ions[22].

The antibacterial effectiveness of chlorapatites strongly rely on the type of doped metals and may be connected with oligodynamic effect. The mechanisms of bactericidal activity of different metal ions are not fully elucidated. There are three main hypothetical mechanisms presented in literature[22]:

(i) ions affecting the production of ATP and DNA replication, after penetration into the bacterial cell;

(ii)   accumulation of ions in the cell membranes consequently changing membrane permeability and disrupting transport;

(iii)   induction of reactive oxygen species (ROSs) by metal ions. All these mechanisms are of great importance in case of eradication of bacterial infection, especially, as the antibiotic resistance amongst pathogenic species is rising.

Chlorapatites compositions tested in this study are multifunctional materials and can be a promising antimicrobial agents, especially chlorapatite doped with europium/silver ions.

---

[22] J. Kolmas, E. Groszyk, and D. Kwiatkowska-Rozycka, *BioMed Research International*, **2014**, 178123.

We took an attempt to elucidate the phenomena of synergic effect for Eu/Ag composition. In accordance to literature, it is suggested that the existence of Eu^{2+} ions could play an important role in the reduction of silver ions as well as a photoluminescence. A spontaneous reduction phenomenon of Eu^{3+} to Eu^{2+} was demonstrated under air condition[23,24,25]. In this case, the influence of Eu^{2+} ions on the Ag^{+} ions was studied. The absorption reflectance spectra of the rare earth ions doped and silver co-doped chlorapatites were measured at 300 K as a function of dopant content (Figure 6). In fact, the representative absorption spectra consist of typical absorption bands of the Eu^{3+} ions with the broad bands in the UV spectral region ascribed to the *4f→5d* transition of Eu^{3+} centred at 48 077 cm^{-1} (208 nm) as well as the charge transfer band (CT) $O^{2-} \rightarrow Eu^{3+}$ centred at 31 446 cm^{-1} (318 nm) whereas an abundance of weak sharp lines were depicted to the intra-configurational *f-f* electron transition of Eu^{3+} ions and finally, silver plasmons centred at 25 641 cm^{-1} (390 nm).
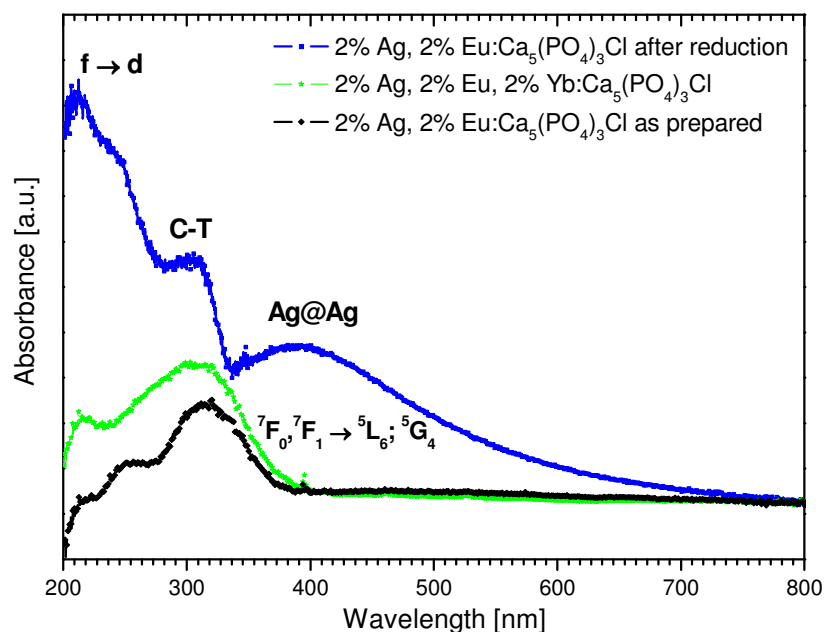

Figure 6. Reflectance absorption spectra of different chlorapatites recorded at 300 K.

[23] Q. Jiao, J. Qiu, D. Zhou, X. Xu, Mater. Res. Bull. 2014, **51**, 315.

[24] R.J. Wiglusz, T. Grzyb, S. Lis and W. Strek, J. Nanosci. Nanotech. 2009, **9**, 5803.

[25] R.J. Wiglusz, T. Grzyb, A. Bednarkiewicz, S. Lis and W. Strek, Eur. J. Inorg. Chem., 2012, **21**, 3418.

The results indicated that the precipitation of Ag^0 could be promoted by the Eu^{2+} ions in chlorapatites with no need of any additional process. Moreover, physical and chemical treatment processes - the reduction of Ag^+ ions to metal atoms (Ag^0) also occurred and Ag^+, Ag^0 can form on the chlorapatites silver aggregates[26]. In other words, the Ag^+ ions reduced with Eu^{2+} ions doping and leads to the antibacterial properties of co-doped nanoparticles (Figure 7). Silver ions alone are not efficient as they are easily removed from the environment. Therefore, the chlorapatites with silver and co-doped with different ions were prepared. Such composites were designed to release silver ions gradually for a long time. Those composite materials are perfect candidate for medical devices with long-term release of antibacterial particles.
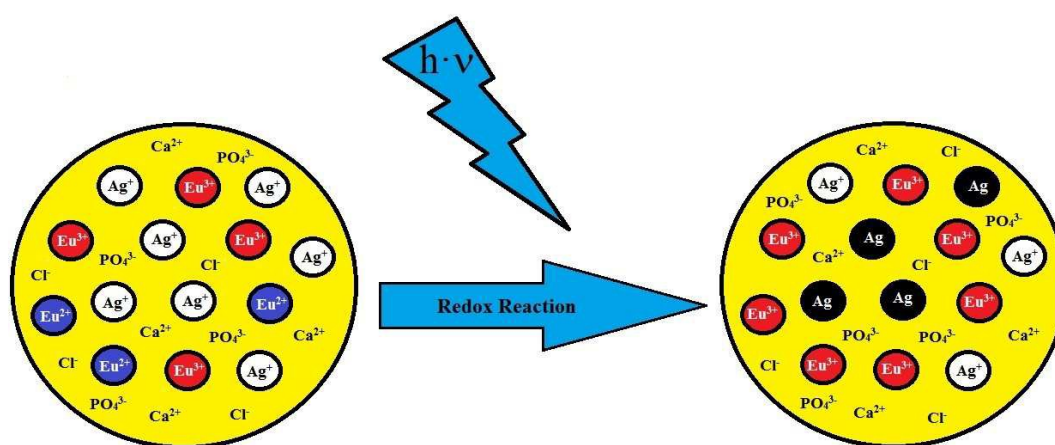

Figure 7. Schematic illustration of reductions as well as oxidation of Eu^{2+} and Ag^+ ions in chlorapatite samples.

Silver ions alone are not efficient as they are easily removed from the environment so the proposed mechanism is crucial for antibacterial properties of testes nanomaterials. The chlorapatites with silver and co-doped with other metal ions were designed to release silver ions gradually for a long period of time. This long process allow to preserve antibacterial properties and use this composite for different medical applications.

[26] L. P. Naranjo, C. B. De Araújo, O. L. Malta, P. A. S. Cruz, and L. R. P. Kassab, Appl. Phys. Lett., 2005, **87**, 241914.

Conclusions

Nanocrystalline chlorapatites activated with lanthanide ions as well as silver ions were successfully prepared using hydrothermal technique as single phased material. Detailed structural study using X-Ray diffraction and Rietveld analysis confirmed complete crystallization and nanocrystalline nature of the samples. Primary size of particles were estimated about 60 nm with fairly broad size distribution.

The microbiological activity of chlorapatites co-doped with lanthanide and silver ions against *E. coli* ATCC11229 and ATCC25922, *K. pneumoniae* ATCC 700603, and *P. aeruginosa* PAO1 and ATCC27853 cultures was demonstrated and the role of dopants and co-dopants was explained. The highest activities against tested Gram-negative bacteria, and concomitantly the highest potential for medical use, were shown for $Ca_{10}(PO_4)_6Cl_2$ compositions doped with Eu^{3+}/Ag^+ and $Eu^{3+}/Ag^+/Yb^{3+}$, where 0.01% concentration eliminated 100% of bacterial cells from treated culture.

Acknowledgements